Письма в ЖЭТФ, том 59, вып.12, стр.816 - 820

BRAGG REFLECTION FROM EQUIDISTANT PLANES OF VORTEX-SHEETS IN ROTATING ^{3}He-A

Ü.Parts[+], *J.H.Koivuniemi*[+], *M.Krusius*[+], *V.M.H.Ruutu*[+], *E.V.Thuneberg*[+], *G.E.Volovik*[+,*]

[+] *Low Temperature Laboratory, Helsinki University of Technology, 02150 Espoo, Finland*

[*] *Landau Institute for Theoretical Physics, RAS 117334, Moscow, Russia*

Submitted May 12, 1994

Recently a new state of rotating superfluid ^{3}He-A was discovered which consists of equidistant planes of vortex sheets. Its cw NMR absorption spectrum includes a small satellite peak which has the largest relative frequency shift ever observed in ^{3}He-A. We interpret this peak to arise from the excitation of a stationary spin wave mode localized in the gaps between the vortex sheets. The mode corresponds to the first Bragg reflection from a 1-dimensional periodic potential. The frequency shift provides a measurement of the distance between vortex sheets. The distance agrees with the prediction of Landau and Lifshitz in 1955.

Many different structures of quantized vorticity have been found to exist in ^{3}He superfluids when they are rotated within a cylindrical container at an angular velocity Ω. Most recently a new state of vorticity has been identified in NMR measurements on the anisotropic ^{3}He-A phase [1]. This state was interpreted to consist of vortex sheets. The sheets are parallel to the rotation axis Ω and are separated by layers of vortex-free superflow. Similar to vortex lines, the sheets allow the solid-body like rotation of the superfluid on a macroscopic scale. The distance b between the sheets, which is determined by the competition of the kinetic energy of the counterflow $\frac{1}{2}\rho_s(\mathbf{v}_s - \mathbf{v}_n)^2$ and the surface tension σ of the sheets, was found by Landau and Lifshitz [2]

$$b = \left(\frac{3\sigma}{\rho_s \Omega^2}\right)^{1/3} \qquad (1)$$

in an attempt to understand the rotating state of superfluid ^{4}He.

The vortex-soliton, which forms the sheet in ^{3}He-A, is a combination of a 2-dimensional domain wall (called soliton) and 1-dimensional vortices. The wall is between domains having parallel ($\hat{\mathbf{l}} = \hat{\mathbf{d}}$) and antiparallel ($\hat{\mathbf{l}} = -\hat{\mathbf{d}}$) orientations of $\hat{\mathbf{l}}$ and $\hat{\mathbf{d}}$. Here $\hat{\mathbf{l}}$ and $\hat{\mathbf{d}}$ are the orbital and magnetic anisotropy axes, respectively. The vorticity accumulated to the soliton is nonsingular, i.e., it arises from an inhomogeneous $\hat{\mathbf{l}}$ texture which is periodic along the vortex sheet in the direction $\perp \Omega$. Estimating the surface tension in our experimental conditions, we can calculate from Eq. (1) that $b \approx 360\,\Omega^{-2/3}\,\mu$m (with Ω in rad/s) [1].

The purpose of this letter is to show that b can be directly extracted from the measurement of the frequencies of three peaks in the NMR absorption spectrum. Fig. 1 displays the cw NMR absorption as a function of excitation frequency in the vortex-sheet state. The frequency of an absorption maximum is conventionally expressed as $\omega^2 = \omega_0^2 + R_\perp^2 \omega_\parallel^2$, where $\omega_0 = \gamma H$ is the Larmor frequency and $\omega_\parallel$ the temperature and pressure dependent longitudinal resonance frequency of the A phase. The dominant peak at $R_\perp = R_0 \approx 1$ originates from the dipole-locked

($\hat{\mathbf{l}} = \pm\hat{\mathbf{d}}$) bulk liquid. The low-frequency satellite peak at $R_\perp^2 = R_b^2 = 0.38$ is the signature of the vortex-soliton [1]. It arises from a spin-wave mode that is localized at the sheet because of the attractive potential caused by dipole unlocking ($\hat{\mathbf{l}} \neq \pm\hat{\mathbf{d}}$).

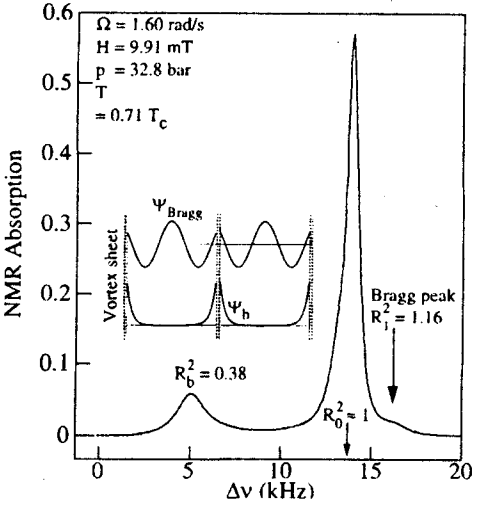

Рис.1

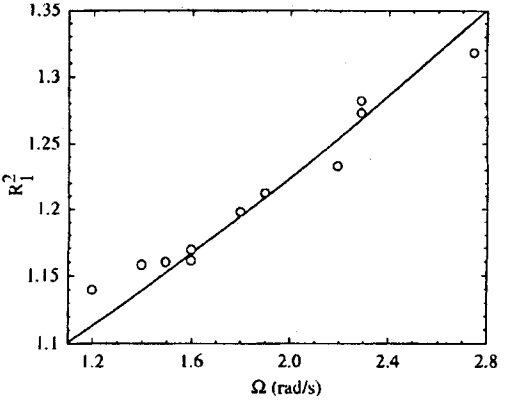

Рис.2

Fig.1. The cw NMR absorption of the vortex-sheet state as a function of the frequency shift $\Delta\nu = \nu - \nu_0$ from the Larmor frequency ν_0. The peak with the lowest frequency R_b arises from a bound state localized on the vortex sheet whereas the other two peaks come from continuum states. The largest peak at R_0 is approximately at the same frequency as the bulk liquid absorption in the nonrotating equilibrium state. Bragg reflections from successive vortex sheets give rise to the small peak at R_1

Fig.2. Measured Ω dependence of the frequency shift R_1^2 of the Bragg peak. The solid line is a fit to the data with $R_1^2 = 1 + 0.090\,\Omega^{4/3}$, which obeys the Ω dependence of Equation (6)

The crucial new feature in Fig. 1 is the smaller satellite at higher frequency $R_\perp^2 = R_1^2 = 1.16$. It is the only clear observation so far of an absorption maximum in the continuum region with $R_\perp > 1$. It can be understood as a Bragg reflection from a 1-dimensional potential, which is created by the periodic sequence of vortex sheets. The Bragg reflection of spin waves from a lattice of vortex lines was originally suggested by Fomin and Kamenskii [3]. We conclude that the reflections from vortex sheets produce larger intensities than from the 2-dimensional vortex lattice because in the latter case no Bragg peak has yet been observed.

The frequency R_b of the low-frequency satellite was found to be independent of Ω. In contrast, the new peak has a frequency R_1 which increases with Ω. In Fig. 2 the measured R_1^2 is plotted as a function of Ω. The result fits the dependence $R_1^2 - 1 = 0.090\Omega^{4/3}$. Also the intensities of the two satellites display opposite Ω dependences: while the intensity of the low-frequency peak increases proportional to the total area of the vortex-soliton $\propto b^{-1} \propto \Omega^{2/3}$, that of the high-frequency maximum decreases with Ω, as shown in Fig. 3. All measurements were done in magnetic field $\mathbf{H} \parallel \Omega \parallel \hat{z}$, and the data analysis is for the temperature $T = 0.71\,T_c$ and pressure $p = 32.8$ bar. The state with vortex sheets was created as described in Ref. [1].

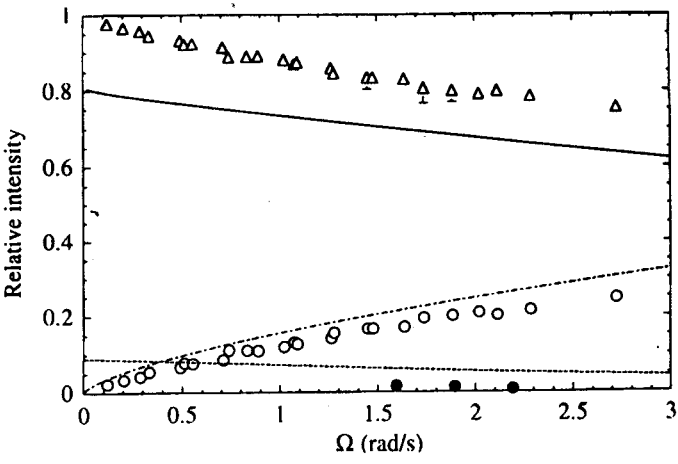

Fig. 3. Integrated NMR absorptions of the 3 peaks in Fig. 1, normalized to the total absorption of the NMR signal, and plotted as a function of Ω: Δ, bulk liquid peak at R_0; o, low-frequency satellite at R_b; and •, high-frequency satellite at R_1. The lines represent Eq. (7) with $a = 1.6\,\xi_{D\perp}$ and $b(\Omega)$ from Fig. 4

The experimental results can be understood semi-quantitatively as follows. Locally the sheets can be considered as planar and we fix $\hat{x}$ as their normal. In our case of $H \parallel \Omega \parallel \hat{z}$ the equilibrium $\hat{d}$ is approximately constant: $\hat{d}_0 \approx \hat{y}$. The NMR excitation makes the spin magnetization to precesses and forces small oscillations of $\hat{d}$ parallel to H: $\hat{d} = \hat{d}_0 + \Psi \hat{z} \cos(\omega t)$. The eigenmodes obey the Schrödinger equation [4, 5]

$$-\xi_{D\perp}^2 \frac{d^2\Psi}{dx^2} + V\Psi = (R_\perp^2 - 1)\Psi, \tag{2}$$

where the dipole length $\xi_{D\perp} = \sqrt{K_6}\,\xi_D \approx 9.8\ \mu$m [6] and the potential $V = -(2\hat{l}_z^2 + \hat{l}_x^2)$. There is a potential well at each sheet whose depth is on the order of unity and range on the order of the soliton thickness $s \sim \xi_{D\perp}$. The thickness s is small compared to the distance b between the sheets; $s \ll b$.

In general, the potential V is known only numerically. The simplest approximation, which we will discuss first, is to assume a delta-function form

$$V(x) = -a \sum_j \delta(x - jb)\,. \tag{3}$$

With this model the bound state is

$$R_b^2 - 1 = -\frac{a^2}{4\xi_{D\perp}^2}\,. \tag{4}$$

Because experimentally $R_b^2 = 0.38$ (Fig. 1), we can extract the potential parameter $a = 1.6\,\xi_{D\perp}$.

Only those eigenstates with nonzero $\int dx\Psi$ couple to the homogeneous NMR excitation. In the continuum these are standing waves of the form $\Psi_n(x) \propto \cos\left(q_n[x - (j + \frac{1}{2})b]\right)$ in the interval $jb < x < (j+1)b$. Here q_n is the n'th positive root of the equation

$$u_n \tan\frac{u_n}{2} = -\gamma\,, \quad \text{with } u_n = q_n b \text{ and } \gamma = \frac{ab}{2\xi_{D\perp}^2}\,. \tag{5}$$

The eigenvalues are $R_n^2 - 1 = \xi_{D\perp}^2 q_n^2$. We see that the main peak, which corresponds to the mode $n = 0$, is slightly shifted to a higher frequency from its position $R_0 = 1$

in a nonrotating liquid. This is also experimentally the case. For the relative shift of the first Bragg peak (mode $n = 1$) we get

$$R_1^2 - R_0^2 = (u_1^2 - u_0^2)\frac{\xi_{D\perp}^2}{b^2} \quad . \tag{6}$$

Taking R_1^2 from Fig. 2, the equations (5) and (6) can be solved self-consistently. In the limit $\Omega \to 0$, where b and γ diverge, the equations are solved simply by $b = \pi\xi_{D\perp}\sqrt{8/(R_1^2 - R_0^2)} \approx 290\Omega^{-2/3}$ μm. The self-consistently calculated $b(\Omega)$ is shown in Fig. 4. It can be fitted as $b \approx 320\,\Omega^{-2/3}$ μm. This is close to the value $b \approx 360\,\Omega^{-2/3}$ μm originally estimated from Eq. (1) in Ref. [1].

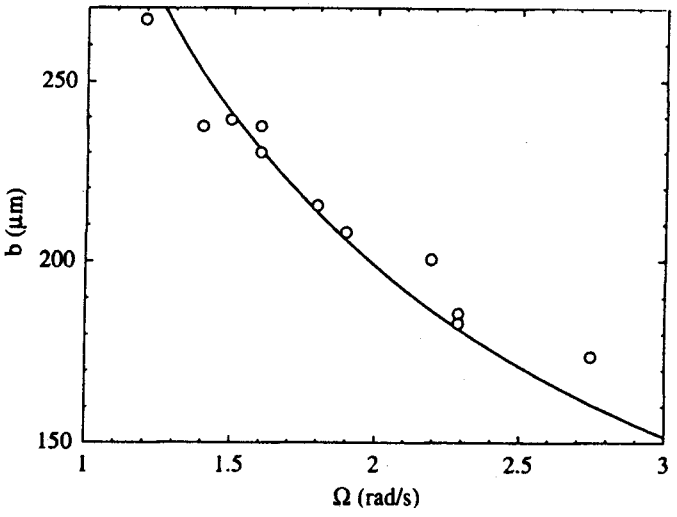

Fig.4. Vortex-sheet separation $b(\Omega)$. The data for the frequency shifts in Figs.1, 2 have been here converted to $b(\Omega)$ using equations (4)-(6). The line is a fit to the $b(\Omega)$ data points with the $\Omega^{-2/3}$ dependence from Eq. (1), giving $b = 320\,\Omega^{-2/3}$ μm (with Ω in rad/s)

The relative intensities of the absorption peaks can be calculated from the formula $I/I_{\rm tot} = (\int dx \Psi)^2/(b\int dx \Psi^2)$. For the 3 absorption peaks we get

$$\frac{I_{\rm b}}{I_{\rm tot}} = 8\frac{\xi_{D\perp}^2}{ab} \quad , \quad \frac{I_0}{I_{\rm tot}} = \frac{8}{u_0^2}\,\frac{\sin^2\frac{u_0}{2}}{1+\frac{\sin u_0}{u_0}} \quad , \quad \frac{I_1}{I_{\rm tot}} = \frac{8}{u_1^2}\,\frac{\sin^2\frac{u_1}{2}}{1+\frac{\sin u_1}{u_1}} \quad . \tag{7}$$

These expressions are compared in Fig. 3 to the measured intensities as a function of Ω. The uncertainty in the measured intensity is smaller than 4 % for the two large peaks while for the high-frequency peak it is on the order of 100 % because of the strong overlap with the main peak. The theoretical and measured intensities of the bound state peak are rather close to each other in spite of the crude model (3). For the Bragg peak the calculated intensity is several times higher than the measured. Its monotonous decrease from the $\Omega \to 0$ limiting value $8/(3\pi)^2$ nevertheless reproduces the experimental behavior.

The delta-function approximation (3) is valid in the limit that the extension of the wave function essentially exceeds the thickness s of a vortex sheet. This is well satisfied for the lowest Bragg states, whose wave-length $\lambda \sim b \gg s$. For the bound state this is marginal because the decay length of the wave function $2\xi_{D\perp}^2/a$ is of the same order as the range of the true potential. The more correct approach is to consider the potential in Eq. (3) only for the modes in the continuum region, while a should be extracted from the integration $a = -\int dx\ V$ over the exact

potential in a vortex-soliton instead of using Eq. (4). One possibility to accomplish this is to take the limit of low velocity $\Omega \to 0$ [1]. We will consider this limit for comparison although the data of the Bragg peak exist only at relatively high velocities $\Omega > 1$ rad/s. The vortex sheet consists of alternating twist and bend textures of $\hat{\mathbf{l}}$. At small Ω the vortices in the sheet are far apart and the twist sections dominate. For the twist section we get $a = 4\xi_D\sqrt{\bar{K}_t} \approx 2.4\xi_{D\perp}$ in the notation of Ref. [6]. This estimate provides an upper limit for a to be achieved at the slowest rotation because the potential is deepest at the twist section. Fitting this to the data gives $b \approx 280\,\Omega^{-2/3}\ \mu$m. The intensity of the bound state in this model is

$$\frac{I_b}{I_{tot}} = \frac{\xi_D\sqrt{\pi\bar{K}_t}}{b}\frac{\Gamma(n+1/2)\Gamma^2(n/2)}{\Gamma(n)\Gamma^2((n+1)/2)}\ , \tag{8}$$

where $n = (\sqrt{1+8K_t/K_6} - 1)/2$. This is by the factor 1.2 larger than the result of the delta-function model plotted in Fig. 3.

Another omission above is that the potential is not constant in the y direction because of the inhomogeneity of the $\hat{\mathbf{l}}$ texture. A proper treatment would require the solution of a 2-dimensional Schödinger equation instead of Eq. (2). The variation of a is on the order of 50% and probably leads to some changes in our numerical results.

The fact that the first Bragg peak can be observed in the NMR spectrum attests to the presence of a well correlated 1-dimensional periodic structure. This is a fundamental property of the vortex-sheet state and a strong argument for its existence. The observation of 1-dimensional periodicity suggests that hydrodynamic collective modes with displacements perpendicular to the Ω axis might be observable, such as the analogue of a Tkachenko shear wave of an ordered vortex line lattice. One-dimensional periodicity exists also in smectic liquid crystals, and there a similar Goldstone mode, a coupled oscillation of the density and the spacing b of consecutive planes, has been observed [7].

This work was supported through the ROTA co-operation plan of the Finnish Academy and the Russian Academy of Sciences. G.E.V. was supported in part by the Russian Foundation for Fundamental Sciences, Grants No. 93-02-02687 and 94-02-03121, and Ü.P. enjoyed a scholarship of the Finnish Cultural Foundation.

---

1. Ü.Parts, E.V.Thuneberg, G.E.Volovik, et al., Phys. Rev. Lett., (in print).
2. L.Landau and E. Lifshitz, Doklady Akademii Nauk (USSR) **100**, 669 (1955).
3. I.A.Fomin and V.G.Kamenskii, Pis'ma ZhETF **35**, 241 (1982) [JETP Lett. **35**, 302 (1982)].
4. K.Maki and P.Kumar, Phys. Rev. B **16**, 182 (1977).
5. For a review see M.M.Salomaa, and G.E.Volovik, Rev. Mod. Phys. **59**, 533 (1987) or A.L. Fetter, in Prog. Low Temp. Phys., ed. D.F.Brewer (Elsevier Publ., 1986), Vol. X, p. 1.
6. A.L.Fetter, J.A.Sauls, and D.L.Stein, Phys. Rev. B **28**, 5061 (1983).
7. S.Chandrasekhar, Liquid crystals (Cambridge University Press, Cambridge, 1977).